

Cheating Suffix: Targeted Attack to Text-To-Image Diffusion Models with Multi-Modal Priors

Dingcheng Yang^{1,2}, Yang Bai^{3,*}, Xiaojun Jia⁴, Yang Liu⁴, Xiaochun Cao⁵, Wenjian Yu^{1,*}

¹Dept. Computer Science & Tech., BNRist, Tsinghua University, Beijing, China.

²RealAI.

³Tencent Security Zhuque Lab.

⁴Nanyang Technological University.

⁵Sun Yat-sen University, Shenzhen.

ydc19@mails.tsinghua.edu.cn, mavisbai@tencent.com, jiaxiaojunq@ gmail.com,

yangliu@ntu.edu.sg, caoxiaochun@mail.sysu.edu.cn, yu-wj@tsinghua.edu.cn

Abstract—Diffusion models have been widely deployed in various image generation tasks, demonstrating an extraordinary connection between image and text modalities. However, they face challenges of being maliciously exploited to generate harmful or sensitive images by appending a specific suffix to the original prompt. Existing works mainly focus on using single-modal information to conduct attacks, which fails to utilize multi-modal features and results in less than satisfactory performance. Integrating multi-modal priors (MMP), i.e. both text and image features, we propose a targeted attack method named MMP-Attack in this work. Specifically, the goal of MMP-Attack is to add a target object into the image content while simultaneously removing the original object. The MMP-Attack shows a notable advantage over existing works with superior universality and transferability, which can effectively attack commercial text-to-image (T2I) models such as DALL-E 3. To the best of our knowledge, this marks the first successful attempt of transfer-based attack to commercial T2I models. Our code is publicly available at <https://github.com/ydc123/MMP-Attack>.

1. INTRODUCTION

In recent years, diffusion models [1, 2] have revolutionized the field of image generation, achieving state-of-the-art results in both the diversity and quality of generated content. The advancement of vision-language models [3] has further enhanced the capabilities of diffusion models, giving rise to novel applications in text-to-image (T2I) generation [4, 5, 6, 7]. However, T2I generation raised up with new adversarial risks recently, showing that the commercial T2I models would be maliciously exploited to generate harmful or sensitive content. Zhuang et al. [8] optimized adversarial suffix to conduct untargeted attack and targeted erasing, namely generating random image content unrelated to the original prompt and omitting a specific category mentioned in the original prompt respectively. Liu et al. [9] explored white-box targeted adversarial attacks, which is impractical for attacking confidential commercial models. Mao et al. [10] explored query-based targeted adversarial attacks. However, they demand a significant number of image generations, not only making it time-consuming but also incurring substantial monetary costs when targeting commercial models.

*corresponding author.



Fig. 1: An illustration of different attacks against the T2I model. The optimized *cheating suffixes* are marked in red, and the object to be erased is marked in blue. Our MMP-Attack conducts a targeted attack by adding a specific target object while eliminating the original object.

To carry out a more practical attack, we explore further into manipulating AI-generated content (AIGC) of T2I diffusion models via a targeted adversarial attack, adding a *cheating suffix* to the original prompt. Different from existing attacks that leverage features in either the text or image domain [8, 9, 11], we propose a targeted attack, introducing the *cheating suffix* to exploit multi-modal features. Our goal is to add a specific target object in the generated image while removing an original object. A gradient-based algorithm is proposed to automatically minimize the distance between the original prompt and the target category (to add) in both text feature space and image feature space, efficiently discovering a cheating suffix and thus manipulating the content generated by T2I diffusion models. This algorithm is named **MMP-Attack** for utilizing **Multi-Modal Priors**. An example is shown in Fig. 1, where the original prompt is ‘a photo of person’, the object to erase is `person` and the target category (to add) is set as `bird`, we optimize and add a cheating suffix ‘wild blers rwby migrant’. After feeding the new prompt to an open-source T2I model Stable Diffusion v1.4 [4], it generates images of a bird instead of a person. Our *cheating suffix* demonstrates stealthiness, as they can easily evade predefined sensitive word databases. This makes them particularly difficult to defend against in practical applications, where filtering user prompts is often used as a simple yet effective defense method.

Surprisingly, experiments also exhibit the superior universality and transferability of our *cheating suffix*. Universality indicates that a suffix searched under a specific prefix can, to some extent, generalize to other prefixes. Transferability indicates that the suffix optimized on an open-source diffusion model can be employed to attack a black-box diffusion model, posing a more severe security threat to commercial T2I models, such as DALL-E 3, considering the reluctance of commercial companies to have the model generate harmful images (violence, nudity, etc). In this paper, our experimental results reveal an attack success rate (ASR) of 50.4% in attacking Stable Diffusion v2.1 using the *cheating suffix* generated on Stable Diffusion v1.4.

The major contributions and results are as follows.

- We systematically explore a strict targeted attack on T2I diffusion models, specifically by adding target objects while removing original objects. We propose an **MMP-Attack** by utilizing multi-modal features for the first time.
- Experimental results indicate that our *cheating suffix* generated by MMP-Attack achieves attack success rates exceeding 81.8% with good stealthiness on two open-source T2I models even with only four tokens, showcasing a notable advantage over existing work.
- Our MMP-Attack reveals practical vulnerabilities due to its superior universality and transferability. The cheating suffix generated on Stable Diffusion v1.4 can even successfully attack DALL-E 3. To the best of our knowledge, this marks the first attempt of transfer-based attack on commercial T2I models.

2. RELATED WORK

2.1 Diffusion Models

Diffusion models have achieved remarkable success in the field of image generation through a learnable step-wise denoising process that transforms a simple Gaussian distribution into the data distribution [1]. Some studies have been proposed to accelerating the image generation process [2, 12]. Beyond the field of image synthesis, diffusion models are widely used in diverse fields, including music generation [13], 3D generation [14] and video generation [15]. Notably, by combining with the visual language model CLIP [3], the diffusion model showcases exceptional prowess in text-to-image generation [4].

2.2 Adversarial Examples in T2I Generation

Adversarial examples are crafted by introducing imperceptible perturbations on input data to compromise the performance of deep neural networks [16, 17, 18, 19, 20]. For T2I models, which take prompt as input and generate images as output, it is important to explore their robustness concerning input prompt. From the perspective of prompt learning, Wen et al. [21] automatically searched for prompts corresponding to a specific content. Liu et al. [9] and Maus et al. [11] searched for a prefix/suffix to concatenate with an existing prompt, which can manipulate the image content of T2I models. Liu et al. [9] performed a white-box attack, but the victim model

it required was often confidential. On the other hand, Maus et al. [11] performed a high-cost query-based attack. The practicality of both approaches is limited. Zhuang et al. [8] assumed that the attacker has access to the CLIP model but is blind to the diffusion module for image generation. Under this assumption, they proposed a *query-free* adversarial attack against T2I models, which employed a genetic algorithm to attack the CLIP model. However, they only considered untargeted attack and targeted erasing (see Fig. 1). In this paper, we follow the setting outlined in [8] but address a more challenging task: targeted attack, specifically by adding target objects while removing original objects in original prompts. Our experimental results demonstrate a significant improvement over [8].

3. METHOD

In this section, we propose MMP-Attack, which leverages multi-modal priors to achieve targeted attacks. We begin by outlining the preliminary of T2I generation. Following, we formulate the targeted attack problem for T2I models. Subsequently, we introduce the optimization objective and the corresponding optimization approach for MMP-Attack. An illustration of our MMP-Attack is shown in Fig. 2.

3.1 Preliminary: Pipeline of T2I Generation

Assuming the vocabulary of candidate tokens is a set $\mathbb{V} = \{w_1, w_2, \dots, w_{|\mathbb{V}|}\}$, an input prompt can be expressed as $s \in \mathbb{V}^*$. A well-trained diffusion model consists of two components: a CLIP model and a generative model G . The CLIP model includes an image encoder F^i , which takes an image as input and outputs a d_{emb} -dimensional image embedding vector. It also includes a token embedder E_ψ and a text encoder F^t , which together embed a text prompt into a d_{emb} -dimensional text embedding vector. Here, $\psi \in \mathbb{R}^{|\mathbb{V}| \times d_{\text{token}}}$ serves as an embedding codebook. For the input prompt s , $E_\psi(s)$ is a matrix of shape $|s| \times d_{\text{token}}$, where $E_\psi(s)_i = \psi_j$, with the condition that $w_j = s_i$. This token embedding matrix $E_\psi(s)$ is then input into the text encoder F^t and embedded as a d_{emb} -dimensional text embedding vector. During the training stage, an image is transformed to an image embedding vector by the image encoder. Simultaneously, its caption (text data) is transformed to a text embedding vector by the token embedder and the text encoder. The distance between the two vectors is minimized to enable the CLIP model to align the image space and text space. During the T2I generation stage, the input prompt s is first embedded into a text embedding vector v by the token embedder and text encoder. Then, it is input into the subsequent generative model G to sample $x \sim G(v)$, where $G(v)$ is a probability distribution conditioned on v , and x represents a sampled image. Thus, the T2I generation from the input prompt s can be understood as a process of sampling from the probability distribution $x \sim G(F^t(E_\psi(s)))$.

3.2 Problem Formulation

Let $s_o \in \mathbb{V}^n$ be the original prompt containing n tokens, and m be the number of tokens in the cheating suffix. The

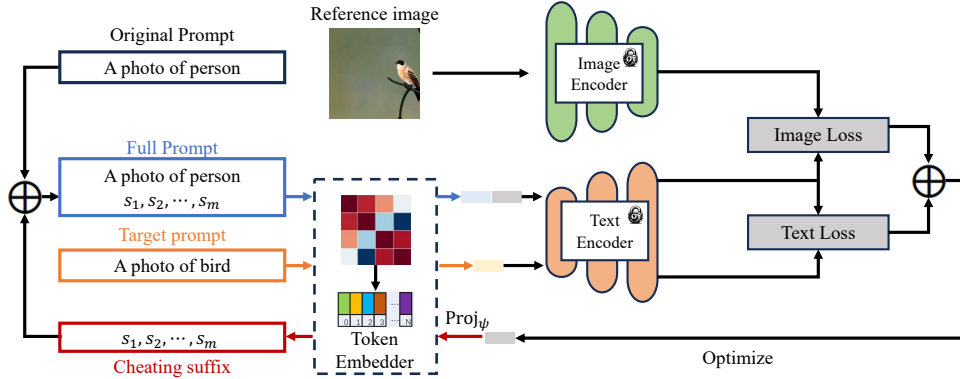


Fig. 2: An illustration of our MMP-Attack pipeline.

cheating suffix to be optimized can be represented as $s_a \in \mathbb{V}^m$, which will be concatenated with s_o to get the full prompt $s_o \oplus s_a \in \mathbb{V}^{n+m}$, where the operator \oplus denotes concatenation operator.

For conducting targeted attacks, we assume that there is a target category $t \in \mathbb{V}$ (e.g., dog, bird, etc.). This target category is irrelevant to the original prompt s_o . We need to search for a cheating suffix that, when concatenated with the original prompt s_o , guides the T2I diffusion model to generate an image containing the target category but is unrelated to s_o . The optimization objective is as follows:

$$\arg\max_{s_a} \mathbb{E}_{x \sim G(F^t(E_\psi(s_o \oplus s_a)))} \mathcal{A}(x, t, s_o), \quad (1)$$

where x represents a randomly generated image based on the full prompt $s_o \oplus s_a$. The $\mathcal{A}(x, t, s_o)$ is an evaluation metric to assess the attack performance. Following the assumptions of relevant work [8], during the optimization process, we have access only to the CLIP model and are blind to the generative model G , which can only be used for evaluating the attack performance of the cheating suffix.

To ensure the naturalness and stealthiness of the cheating suffix, we filtered the vocabulary \mathbb{V} . Firstly, we refined the vocabulary to include only English words that end with the ‘</w>’ symbol, indicating a white-space. This step was necessary because the CLIP vocabulary includes tokens representing prefixes that do not end with </w>, and the concatenation of such tokens could result in the optimized cheating suffix containing non-existent words, thereby reducing the naturalness of the prompt. Secondly, we filtered out the top-20 synonyms of the target category from the vocabulary, to enhance stealthiness and simulate real-world systems that block sensitive words. Specifically, the embedding codebook ψ was employed to define the similarity between two tokens w_i, w_j as $\cos(\psi_i, \psi_j)$, where $\cos(a, b) = \frac{a^T b}{\|a\| \|b\|}$ represents the cosine similarity between two vectors. For example, when the target category t is ‘person’, the top-5 synonyms filtered out include ‘person’, ‘people’, ‘persons’, ‘woman’ and ‘ppl’, respectively. See Appendix A for more details.

3.3 Optimization Objective

Directly solving (1) is infeasible, because it involves a generative model G that is unknown in our assumption. An alternative approach is to first construct a target vector v_t that provides a favorable solution to the following optimization objective:

$$\arg\max_{v_t} \mathbb{E}_{x \sim G(v_t)} \mathcal{A}(x, t, s_o). \quad (2)$$

Assuming such a v_t exists, we can achieve a favorable solution to (1) by maximizing the similarity between the text embedding vectors of $s_o \oplus s_a$ and target vector v_t . Consequently, the optimization objective (1) is transformed into a simplified problem involving only F^i and E_ψ :

$$\arg\max_{s_a} \cos(F^i(E_\psi(s_o \oplus s_a)), v_t). \quad (3)$$

Although G is unknown, constructing a favorable solution for problem (2) is not difficult, since we can use some heuristics solutions. For example, the images generated by a manually crafted prompt $s' = \text{‘a photo of } t \text{’}$ will undoubtedly satisfy the requirements of our targeted attack. Thus, we can utilize its text embedding vector $v_t^{text} = F^t(E_\psi(s'))$ as a target vector to guide the optimization of cheating suffix.

Besides, we integrate image modal information with text modal to better leverage the multi-modal capabilities of T2I models. We propose a target vector based on image modality. Specifically, given a reference image x_t containing the target category, we calculate its image embedding vector $v_t^{image} = F^i(x_t)$, where F^i is the image encoder of the CLIP model. The CLIP model possesses the characteristic that image-text pairs with higher correlation exhibit larger cosine similarities in their embedded vectors, making v_t^{image} be a favorable solution for (2). Finally, we concurrently optimize in both the image and text modalities, where the multi-modal loss is designed as maximizing the similarity between the text embedding vector of $s_o \oplus s_a$ and the two target vectors. The optimization objective is as follows:

$$\begin{aligned} \arg\max_{s_a} \cos(v, v_t^{image}) + \lambda \cos(v, v_t^{text}), \\ \text{s.t. } v = F^i(E_\psi(s_o \oplus s_a)), \end{aligned} \quad (4)$$

where λ is a weighting factor to balance the loss terms between the image and text modalities.

3.4 Optimization Approach

The remaining challenge lies in solving (4). As the optimization variables are defined in a discrete space, it presents a combinatorial optimization problem that is non-differentiable and often NP-hard. To address this issue, a commonly used technique is Straight-Through Estimation (STE) technique [22], which introduces a differentiable function $\text{sg}(\cdot)$ that is defined as the identity function during forward propagation and has zero partial derivatives. It has been previously applied in other discrete optimization domains, including neural network quantization [23, 24], and training discrete generative models such as VQ-VAE [25] and VQ-GAN [26]. Inspired by these works, we leverage the $\text{sg}(\cdot)$ function to solve (4). Specifically, we optimize the token embedding matrix $Z \in \mathbb{R}^{m \times d_{\text{token}}}$ of the cheating suffix, and define a differentiable function $\text{Proj}_{\psi} : \mathbb{R}^{m \times d_{\text{token}}} \rightarrow \mathbb{R}^{m \times d_{\text{token}}}$, where $\text{Proj}_{\psi}(Z)_i = Z_i + \text{sg}(\psi_j - Z_i)$ such that $j = \text{argmin}_{j'} \|\psi_{j'} - Z_i\|_2^2$. Notice that each row in matrix $\text{Proj}_{\psi}(Z)$ corresponds to an entry in the codebook ψ , therefore we can decode the cheating suffix $s_a = E_{\psi}^{-1}(\text{Proj}_{\psi}(Z))$. Moreover, due to the property $E_{\psi}(s_o \oplus s_a) = E_{\psi}(s_o) \oplus E_{\psi}(s_a)$, (4) can be reformulated into the following optimization problem:

$$\begin{aligned} & \text{argmax}_Z \cos(v, v_t^{\text{image}}) + \lambda \cos(v, v_t^{\text{text}}) \\ \text{s.t. } & v = F^i(E_{\psi}(s_o \oplus s_a)) \\ & = F^i(E_{\psi}(s_o \oplus E_{\psi}^{-1}(\text{Proj}_{\psi}(Z)))) \\ & = F^i(E_{\psi}(s_o) \oplus \text{Proj}_{\psi}(Z)). \end{aligned} \quad (5)$$

Because the Proj function is differentiable, (5) can be solved using a gradient-based optimizer, providing better performance compared to prior work [8] that employs a zero-order optimizer. Our optimization approach is summarized in Algorithm 1. The target conditional vectors are first calculated in Step 1-3. Then, the optimization variable Z is initialized and optimized by a gradient descent algorithm (Step 4-13). Finally, the cheating suffix is decoded based on the optimized Z (Step 14).

A good initialization (Step 4) often helps reduce the complexity of the optimization problem, leading to better solutions [27]. To solve (5), we consider three initialization methods:

- 1) **EOS**: Initialize all Z_i as the token embedding for $[\text{eos}]$, where $[\text{eos}]$ is a special token in CLIP vocabulary representing the end of string.
- 2) **Random**: Randomly sample m tokens from the filtered vocabulary and use their embeddings as the initial values for Z .
- 3) **Synonym**: Select the token with the highest cosine similarity to the target category t in the filtered vocabulary, and use its token embedding as the initial values for all Z_i .

The synonym initialization method is used by default, and an ablation study on the initialization method is presented in Section 4.4.

Algorithm 1 MMP-Attack

Input: token embedder E_{ψ} , dimension of the token embedding vector d_{token} , text encoder F^t , image encoder F^i , learning rate η , number of iterations N , original prompt s_o , number of tokens in cheating suffix m , target category $t \in \mathcal{V}$, weighting factor λ , a reference image x_t containing the target category t and unrelated to original prompt s_o .
Output: Cheating suffix s_a .

```

1:  $v_t^{\text{image}} \leftarrow F^i(x_t)$ .
2:  $s' \leftarrow$  ‘a photo of  $t$ ’.
3:  $v_t^{\text{text}} = F^t(E_{\psi}(s'))$ 
4: Initialize  $Z \in \mathbb{R}^{m \times d_{\text{token}}}$ .
5:  $\text{bestloss} \leftarrow \infty, \text{bestZ} \leftarrow Z$ 
6: for  $i \leftarrow 1$  to  $N$  do
7:    $v \leftarrow F^t(E_{\psi}(s_o) \oplus \text{Proj}_{\psi}(Z))$ .
8:    $\mathcal{L} = -\cos(v, v_t^{\text{image}}) - \lambda \cos(v, v_t^{\text{text}})$ .
9:   if  $\text{bestloss} > \mathcal{L}$  then
10:      $\text{bestloss} \leftarrow \mathcal{L}, \text{bestZ} \leftarrow Z$ .
11:   end if
12:    $Z \leftarrow Z - \eta \nabla_Z \mathcal{L}$ .
13: end for
14:  $s_a \leftarrow E_{\psi}^{-1}(\text{Proj}_{\psi}(\text{bestZ}))$ .
```

4. EXPERIMENTAL RESULTS

4.1 Setup

Dataset. Five object categories are selected from the COCO dataset [28], namely car, dog, person, bird, and knife. They are considered as both the original and target categories, forming a total of $5 \times 4 = 20$ distinct category pairs. For each category pair, a cheating suffix is generated. Each cheating suffix is then used to generate 100 images to evaluate the attack performance metrics. The final performance metrics are obtained by averaging across all categories, which means that for a given method, its performance metrics are calculated over $5 \times 4 \times 100 = 2000$ images.

Models. Following the setting in relevant work [8], we initially employ Stable Diffusion v1.4 (SD v14)¹ as the victim model for image generation and performance evaluation. This model utilizes a pretrained CLIP model², which is trained on a dataset containing text-image pairs [29]. Furthermore, we also consider an additional model, Stable Diffusion v2.1 (SD v21)³, which has a distinct CLIP model⁴ compared to SD v14. During image generation, the resolution is set to 512×512 , the number of inference step is set to 50, and the classifier-free guidance scale is set to 7.5. Finally, we also consider a commercial T2I service, i.e., DALL-E 3 [30].

Attack implementation. The Adam optimizer is employed for searching cheating suffix, which are composed of four tokens ($m = 4$). The learning rate is set to 0.001 and the

¹<https://huggingface.co/CompVis/stable-diffusion-v1-4>

²<https://huggingface.co/openai/clip-vit-large-patch14>

³<https://huggingface.co/stabilityai/stable-diffusion-2-1>

⁴<https://huggingface.co/laion/CLIP-ViT-H-14-laion2B-s32B-b79K>

number of optimization iterations is set to 10000. For a single category pair, MMP-Attack takes approximately 6 minutes to run on a single Nvidia RTX 4090 GPU. The synonym initialization method is employed by default, with λ set to 0.1 as the default weighting factor. The reference images used to calculate the loss term for image modality are presented in Appendix A. We consider three baseline methods: 1) **No attack**, meaning no cheating suffix is added; 2) **Random**, where four tokens are randomly chosen to form the cheating suffix; 3) **Genetic**, following the approach in the relevant work [8], we employ a genetic algorithm to search for the cheating suffix.

Evaluation metrics. Given a generated image, the following metrics are considered to evaluate the attacking performance: 1) **CLIP score**: We use the CLIP model to calculate the embedding vectors for the generated image and the prompt ('a photo of t '), subsequently determining their matching score based on cosine similarity. 2) **BLIP score**: BLIP [31] is a better visual-language model. We use it to compute the image-text matching score. 3) **Original Category Non-Detection Rate (OCNDR)**: A binary metric where we employ an object detection model to examine if the generated image fails to detect objects of the original category, indicating an untargeted attack. 4) **Target Category Detection Rate (TCDR)**: Similar to OCNDR, it is a binary metric where we use an object detection model to check if the generated image contains objects of the target category. 5) **BOTH**: A binary metric where the value is 1 if and only if both OCNDR and TCDS are 1. A pretrained faster R-CNN model [32] with a ResNet-50-FPN backbone [33] is utilized as the object detection model to evaluate OCNDR, TCDR and BOTH, which is publicly available at torchvision⁵.

Based on the knowledge of the T2I models, we consider two experimental settings: 1) **Grey-box attack**: In this setting, the generative model G is unknown and we cannot query it. However, we assume that the CLIP model, composed of E_ψ , F^t , and F^i , is known. This assumption arises from the considerable computational cost of training a CLIP model. Consequently, existing diffusion models, such as stable diffusion [4], often leverage an open-source CLIP model. 2) **Black-box attack**: Additionally, we considered a more challenging setting where the CLIP model is also unknown. We adopt a transfer-based attack strategy, where a white-box CLIP model is chosen as surrogate. Subsequently, we leverage this surrogate model to search a cheating suffix. Finally, the searched cheating suffix is employed to attack black-box T2I models. The grey-box setting is adopted to generate cheating suffix directly, while the black-box setting is adopted mainly to evaluate the transferability. **Unless otherwise specified, experiments are conducted within grey-box setting.**

4.2 Effectiveness of MMP-Attack

In this subsection, we demonstrate the effectiveness of MMP-Attack by attacking open-source SD models and com-

paring it with prior work [8]. Zhuang et al. [8] introduced a genetic algorithm for untargeted attacks, aiming to maximize the distance in text feature space from the original prompt. It can be directly extended as a baseline for targeted attack by minimizing the distance in text feature space from the target prompt $s' = \text{'a photo of } t'$. In [8], the number of generation step is set to 50, the number of candidates per step is set to 20, and the length of the cheating suffix is only set to 5 characters. Since this paper focuses on the more challenging targeted attack task, we set the number of generation step to 500. This implies a total of $500 \times 20 = 10000$ forward propagations, which also ensures fairness in computational cost comparison with MMP-Attack. Considering that the cheating suffix in [8] has a length of only 5 characters, which is usually shorter than the length of four tokens we used. To be fair, we additionally consider a stronger baseline. Specifically, we employ the genetic algorithm to search for cheating suffix of length 32. This length exceeds the average character length of cheating suffixes searched by MMP-Attack. We denote these two genetic algorithm-based method as Genetic@5 and Genetic@32, respectively.

Attack results of MMP-Attack and comparative experiments with baselines are listed in Table I. From the table, we can see that all baseline methods exhibit relatively weak attack performance. This highlights the difficulty of the targeted attack problem. Then, Table I also demonstrates a substantial superiority of MMP-Attack over the baselines. Specifically, for the BOTH score, MMP-Attack surpasses the strongest baseline Genetic@32 by 67.6% and 80.9% on SD14 and SD21, respectively. This metric offers an intuitive reflection of attack success rates, requiring the generated images not only exclude the original category but also contain the target category.

TABLE I: Targeted attack results of different methods. 'Genetic' indicates the relevant work [8]. The metrics are defined in Section 4.1. **Best results are boldfaced.**

Model	Method	CLIP	BLIP	OCNDR	TCDR	BOTH
SD v14	No Attack	0.204	0.019	5.0%	1.6%	0.1%
	Random	0.203	0.015	5.4%	1.9%	0.6%
	Genetic@5	0.211	0.072	21.4%	20.8%	13.0%
	Genetic@32	0.223	0.066	19.7%	27.4%	14.2%
	MMP-Attack (ours)	0.265	0.414	92.0%	87.2%	81.8%
SD v21	No Attack	0.204	0.019	5.0%	1.6%	0.1%
	Random	0.203	0.015	5.4%	1.9%	0.6%
	Genetic@5	0.200	0.014	9.2%	5.5%	1.1%
	Genetic@32	0.206	0.021	18.7%	11.1%	5.5%
	MMP-Attack (ours)	0.270	0.429	95.2%	91.0%	86.4%

Then, we present some attack results in Fig. 3, showcasing cheating suffixes discovered by MMP-Attack alongside the generated images. More cheating suffixes are presented in Appendix B. By analyzing these suffixes, we observe that MMP-Attack automatically identifies specific tokens to achieve the attack goal. The identified tokens could be relevant words associated with the target object that were not filtered out during the preprocessing stage. For example, when the categories are car and person, our MMP-Attack can

⁵<https://github.com/pytorch/vision>



Fig. 3: Examples of optimized cheating suffixes (marked in red) and their corresponding generated images.

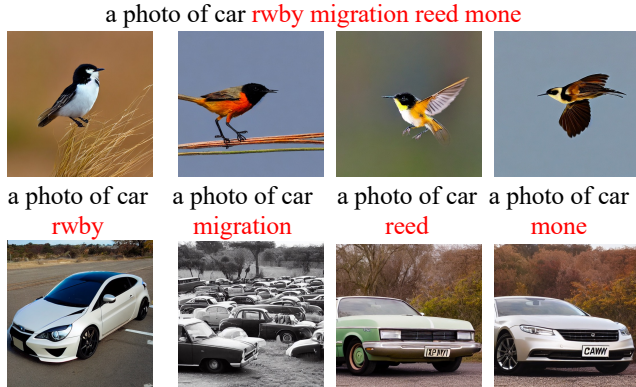


Fig. 4: The images generated by SD v14 using different cheating suffixes (marked in red). The top four images are generated using the cheating suffix we optimized. The bottom four images are respectively generated using each of the four individual tokens as the cheating suffix.

automatically identify relevant tokens such as *buick* and *andre washington*, respectively. The resulting cheating suffixes not only guide the T2I model to generate the desired objects but also lead it to ignore the original prompt. Moreover, in the task of targeting *car* to *bird*, all four tokens are unrelated to birds. Thus, when using *rwby*, *migration*, *reed* and *mone* as cheating suffixes separately, the T2I model generates images of cars (see Fig. 4). However, when using all four tokens simultaneously, it generates images of birds. This constitutes a more imperceptible form of attack, thus bypassing simple filtering-based defense methods.

4.3 Universality and Transferability

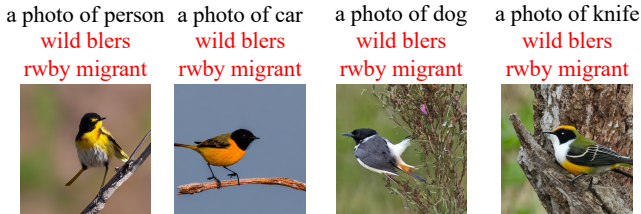


Fig. 5: Examples of universal attacks for SD v14. The cheating suffix marked in red is optimized with the original category *person* and the target category *bird*.

We have shown that, the optimized cheating suffix s_a can overwrite the content of original prompt s_o and generates an image of the target category t . By observing Fig. 3, it can be noticed that the two cheating suffixes discovered for the target category *bird* contain similar tokens, namely both include *rwby*, and one includes *migrate* while the other includes *migration*. This inspires us to explore whether the cheating suffix optimized for one category may be effective for other category pairs within the same target category, referred to as universality. We first attempt to append the cheating suffix ‘*wild blers rwby migrant*’ to *car*, *dog*, and *knife*, and show the generated results in Fig. 5. Surprisingly, even though the original categories are not considered during the optimization process, we find out that targeted attacks still succeeded. Then, we systematically evaluate the universality of 20 cheating suffixes optimized for SD v14. We evaluate their effectiveness in targeted attacks on the other three categories and present the BOTH score in Table II. All cases exhibit a certain degree of universality, with the highest reaching up to 99%.



Fig. 6: Examples of **black-box** targeted attacks. ‘SD v14 → SD v21’ indicates attacking SD v21 using the cheating suffix obtained for attacking SD v14, and vice versa for ‘SD v21 → SD v14’.

TABLE II: Universal attack success rates of MMP-Attack against SD v14. The value in each cell is obtained by averaging BOTH score across the other three categories, excluding the original category (corresponding to the row) and the target category (corresponding to the column), over a total of 3×100 generated images.

	car	person	bird	dog	knife
car	-	66.0%	54.7%	52.3%	88.7%
person	58.3%	-	93.3%	41.3%	89.7%
bird	66.0%	76.7%	-	62.0%	80.7%
dog	39.7%	99.0%	69.3%	-	68.0%
knife	34.0%	63.0%	81.3%	86.3%	-

Adversarial examples have been demonstrated to exhibit transferability, meaning that adversarial examples crafted to attack one model can also be effective against another model. This phenomenon has given rise to transfer-based **black-box** attacks, as discussed in Section 4.1. Next, we conduct experiments to investigate whether the cheating suffixes we optimized also possess such transferability. Below, we use cheating suffixes generated from SD v14 to attack SD v21,

You
a photo of bird hiatus laureate andre washington

You
a photo of knife terriers staffers portrait django

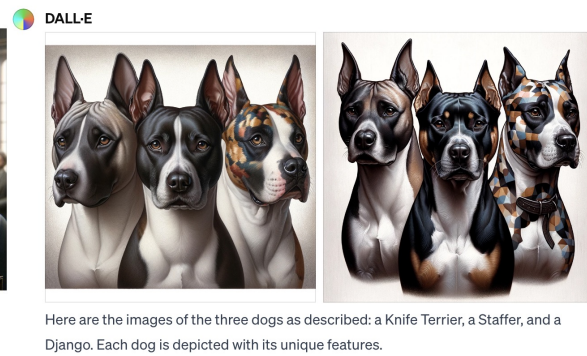
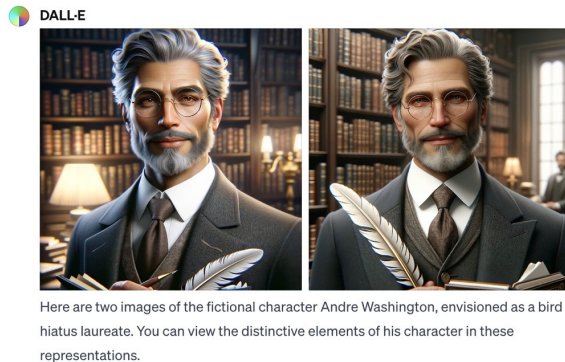


Fig. 7: Examples of **black-box** targeted attacks for the commercial T2I model DALL-E 3. The cheating suffixes are generated by SD v14. (Left) The original category and target category are `person` and `bird`, respectively. (Right) The original category and target category are `knife` and `dog`, respectively.

TABLE III: **Black-box** targeted attack results. ‘SD v14 \rightarrow SD v21’ indicates attacking SD v21 using the cheating suffix obtained for attacking SD v14, and vice versa for ‘SD v21 \rightarrow SD v14’. The metrics are defined in Section 4.1.

Setting	CLIP	BLIP	OCNDR	TCDR	BOTH
SD v14 \rightarrow SD v21	0.243	0.231	72.3%	62.2%	50.4%
SD v21 \rightarrow SD v14	0.247	0.235	71.3%	74.9%	66.8%

and vice versa, use cheating suffixes generated from SD v21 to attack SD v14. The experimental results are listed in Table III, where BOTH scores of 50.4% and 66.8% are achieved for SD v14 and SD v21, respectively. By comparing with Table I, it can be observed that the performance degrades in the black-box attack scenario but still outperforms all the baselines. Some transfer-based attack results are presented in Fig. 6. To the best of our knowledge, prior works on targeted attacks against T2I models have never addressed transferability.

Moreover, we also validated the transferability on the commercial model DALL-E 3, which is a popular T2I online service that can be accessed through ChatGPT 4⁶. Differing from other T2I models, DALL-E 3 automatically refines input prompts to be more user-friendly, mitigating the need for overly complicated prompt engineering. This step increases the difficulty of our transfer-based attacks. Two examples of successful black-box targeted attacks on DALL-E 3 are depicted in Fig. 7. Additionally, we show some black-box attack results conducted on another T2I online service, Imagine Art, in Appendix C.

4.4 Ablation Study

In this subsection, we delve into the crucial aspect of ablation studies, focusing on two key elements that impact the performance of our MMP-Attack: the initialization method and the multi-modal objective functions.

Initialization Methods. We investigate the impact of different initialization methods on attack performance. The three initialization methods introduced in Section 3.4 are considered. We conduct experiments on SD v14 and present the experimental results in Table IV, which shows that the EOS initialization performs the worst. This is because the `[eos]` token is not included in the filtered vocabulary, causing the Proj function to project it onto a distant word at the beginning. This phenomenon will impair the STE technique. In contrast, the ‘Random’ and ‘Synonym’ initialization allow the projection function to degenerate into an identity function at the initial value, enabling STE to provide a sufficiently accurate gradient at the beginning of optimization. Furthermore, the ‘Synonym’ initialization offers a more intuitively better initial solution compared to ‘Random’. Thus, it leads to better results and serves as our default choice.

TABLE IV: Targeted attack results of different initialization methods introduced in Section 3.4 on SD v14. The metrics are defined in Section 4.1. **Best results are boldfaced.**

Initialization	CLIP	BLIP	OCNDR	TCDR	BOTH
EOS	0.262	0.390	82.2%	78.3%	72.3%
Random	0.263	0.400	84.1%	82.0%	74.4%
Synonym	0.265	0.414	92.0%	87.2%	81.8%

Multi-modal Objectives. We further investigate the impact of the weighting factor λ on the attack performance, where λ represent the importance of the text modal loss term. We enumerate different values of λ from $\{0, 0.001, 0.01, 0.1, 0.25, 0.5, 0.75, 1\}$ and plotted the attack results on SD v14 in Fig. 8. When $\lambda = 0$, it implies a method using only the **Image-Modal Prior** (we call it **IMP-Attack**), corresponding to the dashed line. Fig. 8 shows that when λ is small, the attack performance is similar to IMP-Attack, and it increases as λ increases. However, when λ exceeds 0.1, the attack performance starts to decrease rapidly. This phenomenon indicates that the image

⁶<https://chat.openai.com/g/g-2fkFE8rbu-dall-e>

modality plays a more prominent role in MMP-Attack.

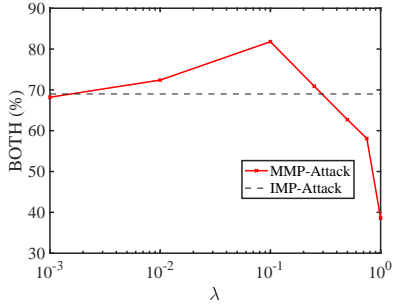


Fig. 8: The BOTH scores versus λ curve. The dashed line indicates an IMP-Attack, using only the image modal prior ($\lambda = 0$).

5. CONCLUSIONS

In this paper, we systematically explore targeted attack to Text-to-Image (T2I) diffusion models in a query-free paradigm by adding specific target objects while removing the original ones. We thoroughly utilize multi-modal priors and propose **MMP-Attack** by incorporating text features and image features. The *cheating suffix* generated by MMP-Attack exhibits extraordinary performance, demonstrating not only stealthiness with high attack success rates but also superior universality and transferability. This enables successful transfer-based attack to commercial T2I models, such as DALL-E 3. Our work contributes to a deeper understanding of T2I generation and establishes a novel paradigm for adversarial studies in AI-generated content. Experimental results showcase the effectiveness and practical applications of our attack in real-world scenarios.

6. IMPACT STATEMENTS

This paper introduces an innovative approach for conducting targeted attacks on text-to-image (T2I) diffusion models. By developing a method to efficiently uncover a ‘cheating suffix’, the research enables manipulation of the image content generated by T2I diffusion models. This work not only contributes to the understanding of vulnerabilities in T2I generation processes but also provides insights into strengthening these systems against potential manipulations.

REFERENCES

- [1] J. Ho, A. Jain, and P. Abbeel, “Denoising diffusion probabilistic models,” *Advances in neural information processing systems*, vol. 33, pp. 6840–6851, 2020.
- [2] J. Song, C. Meng, and S. Ermon, “Denoising diffusion implicit models,” in *International Conference on Learning Representations*, 2020.
- [3] A. Radford, J. W. Kim, C. Hallacy, A. Ramesh, G. Goh, S. Agarwal, G. Sastry, A. Askell, P. Mishkin, J. Clark *et al.*, “Learning transferable visual models from natural language supervision,” in *International conference on machine learning*. PMLR, 2021, pp. 8748–8763.
- [4] R. Rombach, A. Blattmann, D. Lorenz, P. Esser, and B. Ommer, “High-resolution image synthesis with latent diffusion models,” in *Proceedings of the IEEE/CVF conference on computer vision and pattern recognition*, 2022, pp. 10 684–10 695.
- [5] A. Ramesh, P. Dhariwal, A. Nichol, C. Chu, and M. Chen, “Hierarchical text-conditional image generation with clip latents,” *arXiv preprint arXiv:2204.06125*, vol. 1, no. 2, p. 3, 2022.
- [6] A. Q. Nichol, P. Dhariwal, A. Ramesh, P. Shyam, P. Mishkin, B. McGrew, I. Sutskever, and M. Chen, “Glide: Towards photorealistic image generation and editing with text-guided diffusion models,” in *International Conference on Machine Learning*. PMLR, 2022, pp. 16 784–16 804.
- [7] C. Saharia, W. Chan, S. Saxena, L. Li, J. Whang, E. L. Denton, K. Ghasemipour, R. Gontijo Lopes, B. Karagol Ayan, T. Salimans *et al.*, “Photorealistic text-to-image diffusion models with deep language understanding,” *Advances in Neural Information Processing Systems*, vol. 35, pp. 36 479–36 494, 2022.
- [8] H. Zhuang, Y. Zhang, and S. Liu, “A pilot study of query-free adversarial attack against stable diffusion,” in *Proceedings of the IEEE/CVF Conference on Computer Vision and Pattern Recognition*, 2023, pp. 2384–2391.
- [9] Q. Liu, A. Kortylewski, Y. Bai, S. Bai, and A. Yuille, “Intriguing properties of text-guided diffusion models,” *arXiv preprint arXiv:2306.00974*, 2023.
- [10] C. Mao, S. Geng, J. Yang, X. Wang, and C. Vondrick, “Understanding zero-shot adversarial robustness for large-scale models,” in *The Eleventh International Conference on Learning Representations*, 2023.
- [11] N. Maus, P. Chao, E. Wong, and J. R. Gardner, “Black box adversarial prompting for foundation models,” in *The Second Workshop on New Frontiers in Adversarial Machine Learning*, 2023.
- [12] C. Lu, Y. Zhou, F. Bao, J. Chen, C. Li, and J. Zhu, “Dpm-solver: A fast ode solver for diffusion probabilistic model sampling in around 10 steps,” *Advances in Neural Information Processing Systems*, vol. 35, pp. 5775–5787, 2022.
- [13] Q. Huang, D. S. Park, T. Wang, T. I. Denk, A. Ly, N. Chen, Z. Zhang, Z. Zhang, J. Yu, C. Frank *et al.*, “Noise2music: Text-conditioned music generation with diffusion models,” *arXiv preprint arXiv:2302.03917*, 2023.
- [14] Z. Wang, C. Lu, Y. Wang, F. Bao, C. Li, H. Su, and J. Zhu, “Prolificdreamer: High-fidelity and diverse text-to-3d generation with variational score distillation,” in *Advances in Neural Information Processing Systems (NeurIPS)*, 2023.
- [15] A. Blattmann, T. Dockhorn, S. Kulal, D. Mendelevitch, M. Kilian, D. Lorenz, Y. Levi, Z. English, V. Voleti, A. Letts *et al.*, “Stable video diffusion: Scaling latent video diffusion models to large datasets,” *arXiv preprint arXiv:2311.15127*, 2023.

- [16] C. Szegedy, W. Zaremba, I. Sutskever, J. Bruna, D. Erhan, I. Goodfellow, and R. Fergus, "Intriguing properties of neural networks," in *ICLR*, 2014.
- [17] Z. Zhao, Z. Liu, and M. Larson, "On success and simplicity: A second look at transferable targeted attacks," *Advances in Neural Information Processing Systems*, vol. 34, pp. 6115–6128, 2021.
- [18] D. Yang, Z. Xiao, and W. Yu, "Boosting the adversarial transferability of surrogate models with dark knowledge," in *2023 IEEE 35th International Conference on Tools with Artificial Intelligence (ICTAI)*. IEEE, 2023, pp. 627–635.
- [19] Y. Bai, Y. Zeng, Y. Jiang, Y. Wang, S.-T. Xia, and W. Guo, "Improving query efficiency of black-box adversarial attack," in *Computer Vision—ECCV 2020: 16th European Conference, Glasgow, UK, August 23–28, 2020, Proceedings, Part XXV 16*. Springer, 2020, pp. 101–116.
- [20] Y. Bai, Y. Wang, Y. Zeng, Y. Jiang, and S.-T. Xia, "Query efficient black-box adversarial attack on deep neural networks," *Pattern Recognition*, vol. 133, p. 109037, 2023.
- [21] Y. Wen, N. Jain, J. Kirchenbauer, M. Goldblum, J. Geiping, and T. Goldstein, "Hard prompts made easy: Gradient-based discrete optimization for prompt tuning and discovery," in *Thirty-seventh Conference on Neural Information Processing Systems*, 2023.
- [22] Y. Bengio, N. Léonard, and A. Courville, "Estimating or propagating gradients through stochastic neurons for conditional computation," *arXiv preprint arXiv:1308.3432*, 2013.
- [23] D. Yang, W. Yu, H. Mu, and G. Yao, "Dynamic programming assisted quantization approaches for compressing normal and robust dnn models," in *Proceedings of the 26th Asia and South Pacific Design Automation Conference*, 2021, pp. 351–357.
- [24] D. Yang, W. Yu, X. Ding, A. Zhou, and X. Wang, "Dp-nets: Dynamic programming assisted quantization schemes for dnn compression and acceleration," *Integration*, vol. 82, pp. 147–154, 2022.
- [25] A. Van Den Oord, O. Vinyals *et al.*, "Neural discrete representation learning," *Advances in neural information processing systems*, vol. 30, 2017.
- [26] P. Esser, R. Rombach, and B. Ommer, "Taming transformers for high-resolution image synthesis," in *Proceedings of the IEEE/CVF conference on computer vision and pattern recognition*, 2021, pp. 12 873–12 883.
- [27] Y. Tashiro, Y. Song, and S. Ermon, "Diversity can be transferred: Output diversification for white-and black-box attacks," *Advances in neural information processing systems*, vol. 33, pp. 4536–4548, 2020.
- [28] T.-Y. Lin, M. Maire, S. Belongie, J. Hays, P. Perona, D. Ramanan, P. Dollár, and C. L. Zitnick, "Microsoft coco: Common objects in context," in *Computer Vision—ECCV 2014: 13th European Conference, Zurich, Switzerland, September 6-12, 2014, Proceedings, Part V 13*. Springer, 2014, pp. 740–755.
- [29] B. Thomee, D. A. Shamma, G. Friedland, B. Elizalde, K. Ni, D. Poland, D. Borth, and L.-J. Li, "Yfcc100m: The new data in multimedia research," *Communications of the ACM*, vol. 59, no. 2, pp. 64–73, 2016.
- [30] J. Betker, G. Goh, L. Jing, T. Brooks, J. Wang, L. Li, L. Ouyang, J. Zhuang, J. Lee, Y. Guo *et al.*, "Improving image generation with better captions," *Computer Science*. <https://cdn.openai.com/papers/dall-e-3.pdf>, 2023.
- [31] J. Li, D. Li, C. Xiong, and S. Hoi, "Blip: Bootstrapping language-image pre-training for unified vision-language understanding and generation," in *International Conference on Machine Learning*. PMLR, 2022, pp. 12 888–12 900.
- [32] S. Ren, K. He, R. Girshick, and J. Sun, "Faster r-cnn: Towards real-time object detection with region proposal networks," *Advances in neural information processing systems*, vol. 28, 2015.
- [33] T.-Y. Lin, P. Dollár, R. Girshick, K. He, B. Hariharan, and S. Belongie, "Feature pyramid networks for object detection," in *Proceedings of the IEEE conference on computer vision and pattern recognition*, 2017, pp. 2117–2125.

APPENDIX A IMPLEMENTATION DETAILS

Table V lists the words that are filtered out for each target category, as discussed in Section 3.2. The cosine similarity is calculated using a token embedder from Stable Diffusion v1.4. These filtered words are mostly synonyms of the target category, or otherwise words with strong relevance. This filtering process mimics the use of a sensitive word filtering system commonly employed in real-world applications. Fig. 9 illustrates the reference images employed in our experiments, corresponding from left to right to car, dog, person, bird, and knife.

TABLE V: List of filtered words. The first row represents the target category, followed by the next 20 rows representing the corresponding filtered words.

car	dog	person	bird	knife
car	dog	person	bird	knife
cars	dogs	people	birds	knives
vehicle	cat	persons	birdie	fork
vehicles	dawg	woman	tree	sword
dog	doggy	ppl	phone	blade
bus	puppy	guy	fish	wrench
boat	dogg	peoples	cat	gun
automobile	doggo	someone	bee	tool
train	doggie	adult	eagle	guns
van	cats	individual	flight	snakes
bike	horse	thing	birding	inmate
coach	animal	player	horse	cutlery
er	pooch	man	birdman	pistol
sedan	car	member	crow	stabbing
i	dawgs	girl	dot	chair
plane	pup	personal	wildlife	spoon
cat	dad	personality	finch	goalie
phone	adog	somebody	knowledge	bike
road	pet	members	plant	stab
suv	hotdog	child	lizard	skateboard



Fig. 9: Reference images.

APPENDIX B DISPLAY OF ALL SEARCHED CHEATING SUFFIXES

We present all the discovered cheating suffixes on SD v14 and SD v21 in Table VI.

TABLE VI: All results of searched cheating suffixes. ‘Ori. Cat.’ means ‘Original Category’.

Model	Ori. Cat.	car	person	bird	dog	knife
SD v14	car	transmission solved belonged coupe	physician qualified darryl atf	rwby migration reed mone	mutt portrait scout lao	skinner buck durable dagger
	bird	fiercely buick solved belonged	hiatus laureate andre washington	wild biers rwby migrant	analog mutt pocket wilbur	crafted smoked durable gerber
	dog	lewes automotive deluxe survives	hall actor transitions denzel	moth frid rwby tit	since kiddo chihuahua gge	gerber outdoor laminated dagger
	knife	wartime neglected automotive wagon	denzel bipolar libertarian peterson	favorable bul reed tit	terriers staffers portrait django	gazaundertack rosewood transitional gerber
SD v21	car	creole dub oldsmobile extinct	dialogue resident ronald coleman	brian cumin tern hummingbird	tongue nose pied terrier	dmitry authentic pland bowie
	bird	unsolved creole forged automotive	tions founder willie renece	jharkhand tern finch migration	chihuahua shout merit terrier	pioneer hunter finn cutlery
	dog	lyle pontiac creole automotive	voices fellows melvin browne	vo tern detached finch	boston chihuahua photography shout	hunter bur exam bowie
	knife	protected creole oldsmobile abroad	african equity veterans actor	flax programme tree finch	tongue pied chihuahua terrier	authentic topaz hunter petty

APPENDIX C BLACK-BOX TARGETED ATTACK RESULTS ON IMAGINE ART

Additionally, we conducted experiments of black-box targeted attacks on another commercial T2I online service, Imagine Art⁷. Some of the results are shown in Fig. 10.

⁷<https://www.imagine.art/>

a photo of person
wild blers rwby migrant



a photo of bird
fiercely buick solved belonged



a photo of person
analog mutt pocket wilbur



a photo of knife
terriers staffers portrait django



a photo of car
skinner buck durable dagger



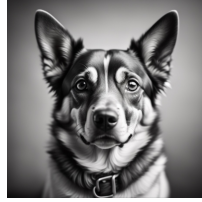
a photo of knife
wartime neglected automotive wagon



a photo of car
mutt portrait scout lao



a photo of person
analog mutt pocket wilbur



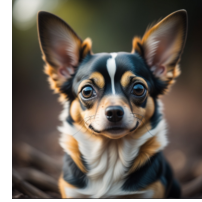
a photo of dog
lewes automotive deluxe survives



a photo of bird
gerber outdoor laminated dagger



a photo of bird
since kiddo chihuahua gge



a photo of person
transmission solved belonged coupe



Fig. 10: Examples of **black-box** targeted attacks on Imagine Art. All the cheating suffixes are generated from SD v14.